Continuous-time model identification for rotorcraft dynamics ⋆

M. Sguanci * **M. Bergamasco** * **M. Lovera** *

* *Dipartimento di Elettronica e Informazione, Politecnico di Milano Piazza Leonardo da Vinci, 32, 20133 Milano, Italy (e-mail: bergamasco,lovera@elet.polimi.it)*

Abstract: Accurate dynamic modelling of helicopter aeromechanics is becoming increasingly important, as progressively stringent requirements are being imposed on rotorcraft control systems. System identification plays an important role as an effective approach to the problem of deriving or fine tuning mathematical models for purposes such as handling qualities assessment and control system design. In this paper the problem of deriving continuous-time models for the dynamics of a small-scale quadrotor helicopter is considered. More precisely, the continuous-time predictor-based subspace identification approach is adopted and the results obtained in an experimental study are presented and discussed.

1. INTRODUCTION

The derivation of accurate dynamic models for helicopter aeromechanics is becoming more and more important, as progressively stringent requirements are being imposed on rotorcraft control systems: as the required control bandwidth increases, accurate models becomes a vital part of the design problem. In this respect, system identification has been known for a long time as a viable approach to the derivation of control-oriented dynamic models in the rotorcraft field (see for example the survey paper Hamel and Kaletka [1997], the recent books Tischler and Remple [2006], Jategaonkar [2006] and the references therein).

In the system identification literature, on the other hand, one of the main novelties of the last two decades has been the development of Subspace Model Identification (SMI) methods (see, e.g., Van Overschee and De Moor [1996], Verhaegen and Verdult [2007]), which have proved extremely successful in dealing with the estimation of state space models for MIMO systems. Surprisingly enough, until recently these methods have received limited attention from the rotorcraft community, with the partial exception of some contributions such as Verhaegen and Varga [1994], Bittanti and Lovera [1997], Lovera [2003]). SMI methods are particularly well suited for rotorcraft problems, for a number of reasons. First of all, the subspace approach can deal in a very natural way with MIMO problems; in addition, all the operations performed by subspace algorithms can be implemented with numerically stable and efficient tools from numerical linear algebra. Finally, information from separate data sets (such as generated during different experiments on the system) can be merged in a very simple way into a single state space model. Recently, see Li and I. [2011], the interest in SMI for helicopter model identification has been somewhat revived and the performance of subspace methods has been demonstrated on flight test data. However, so far only methods and tools which go back 10 to 15 years in the SMI literature (such as the MOESP algorithm of Verhaegen [1994] and the bootstrap-based method for uncertainty analysis of Bittanti and Lovera [2000]) have been considered. Therefore, the further potential benefits offered by the latest developments in the field have not been fully exploited. Among other things, present-day approaches can provide unbiased model estimates from data generated during closed-loop operation, as is frequently the case in experiments for rotorcraft identification (see, e.g., Chiuso and Picci [2005], Huang et al. [2005]) and the direct estimation of continuous-time models from (possibly non-uniformly) sampled input-output data (see Bergamasco and Lovera [2010a,b, 2011] and the references therein).

In view of the above discussion, the aim of the proposed paper is to demonstrate by means of an experimental case study the applicability of SMI methods to the identification of a small-scale quadrotor helicopter (see, e.g., Castillo et al. [2005] for a general introduction to the modelling and control of quadrotors and La Civita et al. [2002], Derafa et al. [2006] for recent references on model identification of rotorcraft UAVs). More precisely, the continuous-time predictor-based subspace identification approach proposed in Bergamasco and Lovera [2010a,b, 2011] is applied to flight data collected during dedicated identification experiments and a model for the hovering quadrotor is derived.

2. QUADROTOR MODELLING AND IDENTIFICATION

Quadrotors are helicopter provided with four rotors (see Figure 1), operated running clockwise and counterclockwise in pairs, so that the net effect of gyroscopic effects and aerodynamic torques in trim conditions is minimised. The vertical motion is controlled by thrusting the four rotors simultaneously, while pitch and roll are commanded by increasing/decreasing the speed of the rear/front and left/right rotors. Finally, yaw control is obtained by com-

⋆ The research has been supported by the MIUR project "New methods for Identification and Adaptive Control for Industrial Systems" and by the AWPARC research contract "Time- and frequency-domain rotorcraft model identification for flight dynamics applications".

Preprint submitted to 16th IFAC Symposium on System Identification.
Received November 14, 2011.

bining the two above actions in a coordinated way. The quadrotor architecture is a very popular one for the development of rotorcraft UAV platforms (see, e.g., Castillo et al. [2005] and the references therein), in view of its favorable dynamic characteristics (see Das et al. [2009]): indeed, although open-loop unstable, like most rotorcraft architectures, quadrotors exhibit a good degree of decoupling, which makes them easier to control. Mathematical models for the dynamics of quadrotors are relatively easy to establish as far the kinematics and dynamics of linear and angular motion are concerned. Characterising aerodynamic effects and additional dynamics such as, e.g., the response of the controlled angular rates of the individual rotors, is far from trivial, and has led to the development of many approaches to the experimental characterisation of the overall dynamic response of the quadrotor. In this paper, the following input and output variables are considered. Since the forces and moments generated by the rotors are quadratic functions of the rotors angular rates (see, e.g., Castillo et al. [2005]), a change of variables is usually adopted to define control inputs which enter linearly the equations of motion, namely

$$u = [u_{col}\ u_{lon}\ u_{lat}\ u_{ped}]^T = \begin{bmatrix} \Omega_1^2 + \Omega_2^2 + \Omega_3^2 + \Omega_4^2 \\ \Omega_4^2 - \Omega_2^2 \\ \Omega_3^2 - \Omega_1^2 \\ \Omega_2^2 + \Omega_4^2 - \Omega_1^2 - \Omega_3^2 \end{bmatrix},$$

where Ω_i, $i = 1, \ldots, 4$ are the angular rates of the four rotors, u_{col} can be interpreted as a force along the vertical body axis and u_{lon}, u_{lat} and u_{ped} as, respectively, a pitching, rolling and a yawing moment around the body axes. The output vector on the other hand includes the measurements provided by the available inertial sensors, i.e., $y = [a_x\ a_y\ a_z\ p\ q\ r]^T$, where a_x, a_y and a_z are the measurements of the acceleration along the three body axes and p, q and r are, respectively, the measurements of the components of the quadrotor's angular rate, again expressed in the body frame.

Fig. 1. The Mikrokopter quadrotor used in this study.

3. CONTINUOUS-TIME PREDICTOR-BASED SUBSPACE MODEL IDENTIFICATION

Consider the linear, time-invariant continuous-time system

$$\begin{aligned} dx(t) &= Ax(t)dt + Bu(t)dt + dw(t),\ x(0) = x_0 \\ dz(t) &= Cx(t)dt + Du(t)dt + dv(t) \\ y(t)dt &= dz(t) \end{aligned} \tag{1}$$

where $x \in \mathbb{R}^n$, $u \in \mathbb{R}^m$ and $y \in \mathbb{R}^p$ are, respectively, the state, input and output vectors and $w \in \mathbb{R}^n$ and $v \in \mathbb{R}^p$ are the process and the measurement noise, respectively, modelled as Wiener processes with incremental covariance given by

$$E\left\{ \begin{bmatrix} dw(t) \\ dv(t) \end{bmatrix} \begin{bmatrix} dw(t) \\ dv(t) \end{bmatrix}^T \right\} = \begin{bmatrix} Q & S \\ S^T & R \end{bmatrix} dt.$$

The system matrices A, B, C and D, of appropriate dimensions, are such that (A, C) is observable and $(A, [B, Q^{1/2}])$ is controllable. Assume that a dataset $\{u(t_i), y(t_i)\}$, $i \in [1, N]$ of sampled input/output data (possibly associated with a non equidistant sequence of sampling instants) obtained from system (1) is available. Then, the problem is to provide an estimate of the state space matrices A, B, C and D (up to a similarity transformation) on the basis of the available data. In the following a number of definitions will be used, which are summarised hereafter for the sake of clarity. See, e.g., Zhou et al. [1996], Johansson et al. [1999], Ohta [2005] for further details. Let $\mathcal{L}_2(0, \infty)$ denote the space of square integrable and Lebesgue measurable functions of time $0 < t < \infty$.

Consider the first order all-pass (inner) transfer function

$$w(s) = \frac{s-a}{s+a}, a > 0. \tag{2}$$

$w(s)$ generates the family of Laguerre filters, defined as

$$\mathcal{L}_i(s) = w^i(s)\mathcal{L}_0(s) = \sqrt{2a}\frac{(s-a)^i}{(s+a)^{i+1}}. \tag{3}$$

Denote with $\ell_i(t)$ the impulse response of the i-th Laguerre filter. Then, it can be shown that the set

$$\{\ell_0, \ell_1, \ldots, \ell_i, \ldots\} \tag{4}$$

is an orthonormal basis of $\mathcal{L}_2(0, \infty)$, i.e., all signals in $\mathcal{L}_2(0, \infty)$ can be represented by means of the set of their projections on the Laguerre basis. Under the above assumptions, (1) can be written in innovation form as

$$\begin{aligned} dx(t) &= Ax(t)dt + Bu(t)dt + Kde(t) \\ dz(t) &= Cx(t)dt + Du(t)dt + de(t) \\ y(t)dt &= dz(t), \end{aligned} \tag{5}$$

and it is possible to apply the results of Ohta and Kawai [2004] to derive a discrete-time equivalent model, as follows. Consider the first order inner function $w(s)$ and apply to the input u, the output y and the innovation e of (5) the transformations

$$\begin{aligned} \tilde{u}(k) &= \int_0^\infty \ell_k(t)u(t)dt \\ \tilde{y}(k) &= \int_0^\infty \ell_k(t)y(t)dt \\ \tilde{e}(k) &= \int_0^\infty \ell_k(t)e(t)dt, \end{aligned} \tag{6}$$

where $\tilde{u}(k) \in \mathbb{R}^m$, $\tilde{e}(k) \in \mathbb{R}^p$ and $\tilde{y}(k) \in \mathbb{R}^p$. Then (see Ohta and Kawai [2004] for details) the transformed system has the state space representation

$$\begin{aligned} \xi(k+1) &= A_o\xi(k) + B_o\tilde{u}(k) + K_o\tilde{e}(k),\ \xi(0) = 0 \\ \tilde{y}(k) &= C_o\xi(k) + D_o\tilde{u}(k) + \tilde{e}(k) \end{aligned} \tag{7}$$

where the state space matrices are given by

$$\begin{aligned} A_o &= (A-aI)^{-1}(A+aI) \\ B_o &= \sqrt{2a}(A-aI)^{-1}B \\ C_o &= -\sqrt{2a}C(A-aI)^{-1} \\ D_o &= D - C(A-aI)^{-1}B. \end{aligned} \tag{8}$$

Starting from system (7), a PBSID-like approach to the estimation of the state space matrices A_o, B_o, C_o, D_o, K_o can be derived. Considering the sequence of sampling instants t_i, $i = 1, \dots, N$, the input u, the output y and the innovation e of (5) are subjected to the transformations

$$\begin{aligned} \tilde{u}_i(k) &= \int_0^\infty \ell_k(\tau)u(t_i+\tau)d\tau \\ \tilde{y}_i(k) &= \int_0^\infty \ell_k(\tau)y(t_i+\tau)d\tau \\ \tilde{e}_i(k) &= \int_0^\infty \ell_k(\tau)e(t_i+\tau)d\tau \end{aligned} \tag{9}$$

(or to the equivalent ones derived from (6)), where $\tilde{u}_i(k) \in \mathbb{R}^m$, $\tilde{e}_i(k) \in \mathbb{R}^p$ and $\tilde{y}_i(k) \in \mathbb{R}^p$. Then (see Ohta and Kawai [2004] for details) the transformed system has the state space representation

$$\begin{aligned} \xi_i(k+1) &= A_o\xi_i(k) + B_o\tilde{u}_i(k) + K_o\tilde{e}_i(k),\ \xi_i(0) = x(t_i) \\ \tilde{y}_i(k) &= C_o\xi_i(k) + D_o\tilde{u}_i(k) + \tilde{e}_i(k) \end{aligned} \tag{10}$$

where the state space matrices are given by (8).

Letting now

$$\tilde{z}_i(k) = \left[\tilde{u}_i^T(k)\ \tilde{y}_i^T(k)\right]^T$$

and

$$\bar{A}_o = A_o - K_oC_o, \quad \bar{B}_o = B_o - K_oD_o, \quad \widetilde{B}_o = \left[\bar{B}_o\ K_o\right],$$

system (10) can be written as

$$\begin{aligned} \xi_i(k+1) &= \bar{A}_o\xi_i(k) + \widetilde{B}_o\tilde{z}_i(k),\ \xi_i(0) = x(t_i) \\ \tilde{y}_i(k) &= C_o\xi_i(k) + D_o\tilde{u}_i(k) + \tilde{e}_i(k), \end{aligned} \tag{11}$$

to which the PBSID$_{opt}$ algorithm can be applied to compute estimates of the state space matrices A_o, B_o, C_o, D_o, K_o. To this purpose note that iterating $p-1$ times the projection operation (i.e., propagating $p-1$ forward in the index k the first of equations (11), where p is the so-called past window length) one gets

$$\begin{aligned} \xi_i(k+2) &= \bar{A}_o^2\xi_i(k) + \left[\bar{A}_o\widetilde{B}_o\ \widetilde{B}_o\right]\begin{bmatrix}\tilde{z}_i(k) \\ \tilde{z}_i(k+1)\end{bmatrix} \\ &\vdots \\ \xi_i(k+p) &= \bar{A}_o^p\xi_i(k) + \mathcal{K}^pZ_i^{0,p-1} \end{aligned} \tag{12}$$

where

$$\mathcal{K}^p = \left[\bar{A}_o^{p-1}\widetilde{B}_0\ \dots\ \widetilde{B}_o\right] \tag{13}$$

is the extended controllability matrix of the system in the transformed domain and

$$Z_i^{0,p-1} = \begin{bmatrix}\tilde{z}_i(k) \\ \vdots \\ \tilde{z}_i(k+p-1)\end{bmatrix}.$$

Under the considered assumptions, $\bar{A}_o$ has all the eigenvalues inside the open unit circle, so the term $\bar{A}_o^p\xi_i(k)$ is negligible for sufficiently large values of p and we have that

$$\xi_i(k+p) \simeq \mathcal{K}^pZ_i^{0,p-1}.$$

As a consequence, the input-output behaviour of the system is approximately given by

$$\begin{aligned} \tilde{y}_i(k+p) &\simeq C_o\mathcal{K}^pZ_i^{0,p-1} + D_o\tilde{u}_i(k+p) + \tilde{e}_i(k+p) \\ &\vdots \\ \tilde{y}_i(k+p+f) &\simeq C_o\mathcal{K}^pZ_i^{f,p+f-1} + D_o\tilde{u}_i(k+p+f)+ \\ &\quad + \tilde{e}_i(k+p+f), \end{aligned} \tag{14}$$

so that introducing the vector notation

$$\begin{aligned} Y_i^{p,f} &= [\tilde{y}_i(k+p)\ \tilde{y}_i(k+p+1)\ \dots\ \tilde{y}_i(k+p+f)] \\ U_i^{p,f} &= [\tilde{u}_i(k+p)\ \tilde{u}_i(k+p+1)\ \dots\ \tilde{u}_i(k+p+f)] \\ E_i^{p,f} &= [\tilde{e}_i(k+p)\ \tilde{e}_i(k+p+1)\ \dots\ \tilde{e}_i(k+p+f)] \\ \Xi_i^{p,f} &= [\xi_i(k+p)\ \xi_i(k+p+1)\ \dots\ \xi_i(k+p+f)] \\ \bar{Z}_i^{p,f} &= \left[Z_i^{0,p-1}\ Z_i^{1,p}\ \dots\ Z_i^{f,p+f-1}\right] \end{aligned} \tag{15}$$

equations (12) and (14) can be rewritten as

$$\begin{aligned} \Xi_i^{p,f} &\simeq \mathcal{K}^p\bar{Z}_i^{p,f} \\ Y_i^{p,f} &\simeq C_o\mathcal{K}^p\bar{Z}_i^{p,f} + D_oU_i^{p,f} + E_i^{p,f}. \end{aligned} \tag{16}$$

Considering now the entire dataset for $i = 1, \dots, N$, the data matrices become

$$\begin{aligned} Y^{p,f} = [&\tilde{y}_1(k+p)\dots\tilde{y}_N(k+p)\dots \\ &\tilde{y}_1(k+p+f)\dots\tilde{y}_N(k+p+f)], \end{aligned} \tag{17}$$

and similarly for $U_i^{p,f}$, $E_i^{p,f}$, $\Xi_i^{p,f}$ and $\bar{Z}_i^{p,f}$. The data equations (16), in turn, are given by

$$\begin{aligned} \Xi^{p,f} &\simeq \mathcal{K}^p\bar{Z}^{p,f} \\ Y^{p,f} &\simeq C_o\mathcal{K}^p\bar{Z}^{p,f} + D_oU^{p,f} + E^{p,f}. \end{aligned} \tag{18}$$

From this point on, the algorithm can be developed along the lines of the discrete-time PBSID$_{opt}$ method, i.e., by carrying out the following steps. Considering $p = f$, estimates for the matrices $C_o\mathcal{K}^p$ and D_o are first computed by solving the least-squares problem

$$\min_{C_o\mathcal{K}^p, D_o} \|Y^{p,p} - C_o\mathcal{K}^p\bar{Z}^{p,p} - D_oU^{p,p}\|_F. \tag{19}$$

Defining now the extended observability matrix Γ^p as

$$\Gamma^p = \begin{bmatrix} C_o \\ C_o\bar{A}_o \\ \vdots \\ C_o\bar{A}_o^{p-1} \end{bmatrix} \tag{20}$$

and noting that the product of Γ^p and $\mathcal{K}^p$ can be written as

$$\Gamma^p\mathcal{K}^p \simeq \begin{bmatrix} C_o\bar{A}^{p-1}\widetilde{B}_o & \dots & C_o\widetilde{B}_o \\ 0 & \dots & C_o\bar{A}\widetilde{B}_o \\ \vdots & & \\ 0 & \dots & C_o\bar{A}^{p-1}\widetilde{B}_o \end{bmatrix}, \tag{21}$$

such product can be computed using the estimate $\widehat{C_o\mathcal{K}^p}$ of $C_o\mathcal{K}^p$ obtained by solving the least squares problem (19).

Recalling now that

$$\Xi^{p,p} \simeq \mathcal{K}^p\bar{Z}^{p,p} \tag{22}$$

it also holds that

$$\Gamma^p\Xi^{p,p} \simeq \Gamma^p\mathcal{K}^p\bar{Z}^{p,p}. \tag{23}$$

Therefore, computing the singular value decomposition

$$\Gamma^p\mathcal{K}^p\bar{Z}^{p,p} = U\Sigma V^T \tag{24}$$

an estimate of the state sequence can be obtained as

$$\widehat{\Xi}^{p,p} = \Sigma_n^{1/2}V_n^T = \Sigma_n^{-1/2}U_n^T\Gamma^p\mathcal{K}^p\bar{Z}^{p,p}, \tag{25}$$

Preprint submitted to 16th IFAC Symposium on System Identification.
Received November 14, 2011.

from which, in turn, an estimate of C_o can be computed by solving the least squares problem

$$\min_{C_o} \|Y^{p,p} - \widehat{D}_o U^{p,p} - C_o \widehat{\Xi}^{p,p}\|_F. \tag{26}$$

The final steps consist of the estimation of the innovation data matrix $E^{p,p}$

$$E^{p,p} = Y^{p,p} - \widehat{C}_o \widehat{\Xi}^{p,p} - \widehat{D}_o U^{p,p} \tag{27}$$

and of the entire set of the state space matrices for the system in the transformed domain, which can be obtained by solving the least squares problem

$$\min_{A_o, B_o, K_o} \|\widehat{\Xi}^{p+1,p} - A_o \widehat{\Xi}^{p,p-1} - B_o U^{p,p-1} - K_o E^{p,p-1}\|_F. \tag{28}$$

Remark 1. Since the dynamics of the quadrotor is open-loop unstable, in order to validate the identified models the estimation of the initial state is necessary. This problem can be faced in the framework of the above described identification algorithm, as follows. The estimation is performed considering the simulation of the system model (1) where the estimated matrices are used and the noise is not taken into account. Under these assumptions the output at each time instant t is given by

$$y(t) = Ce^{A(t-t_0)}x_0 + C\int_{t_0}^{t} e^{A(t-\tau)}Bu(\tau)d\tau + Du(t). \tag{29}$$

Therefore given the input and output data it is possible to solve a least squares problem to obtain an estimate of x_0.

Remark 2. As is frequently the case with SMI algorithms, also the approach outlined above can use data gathered in different experiments simultaneously. Assuming that M datasets are available, they are independently projected using the transformation (9). The matrix $Y^{p,p}$ is then built as

$$Y^{p,p} = \left[Y^{p,p,1} \; Y^{p,p,\cdots} \; Y^{p,p,M} \right], \tag{30}$$

and similarly for the construction of $U^{p,p}$ and $\bar{Z}^{p,p}$.

4. IDENTIFICATION-ORIENTED FLIGHT TESTING

4.1 The experimental setup

The quadrotor used in this work is a modified version of the Mikrokopter platform, an open source project developed and distributed by HiSystems GmbH (Germany). The Mikrokopter consists of a frame composed by four tubes held together by a metal cross as shown in Figure 1, with the four motors placed at the end of the tubes. The onboard electronics are piled up at the centre of the cross in order to maintain a good mass distribution. The size of the quadrotor is approximately 45 × 45 × 20 cm and its mass is about 1 kg (with battery). The quadrotor is powered with a Lithium-ion polymer battery (11.1 V, 2200 mAh) that guarantees an autonomy of about 15 minutes. The original design provides three electronic boards:

Flight-Ctrl It is the main board of the quadrotor. It includes the AVR Atmel 8-bit microcontroller (20 MHz), a set of three MEMS accelerometers and a set of three gyroscopes. This board is the flight controller, indeed it uses the measurements of the sensors and the command inputs taken through the receiver to set the motors speed rates in the proper way. The sensors outputs are sampled using the internal ADC with a 10 bits resolution.

BL-Ctrl (x4) It is the driver of the motor. The microcontroller mounted on this board is an AVR Atmel 8-bit (8MHz) and it is dedicated to the generation of the PWM signal in order to control the motor angular rate according to the set-point communicated through the Inter Integrated Circuit (I^2C) bus by the Flight-Ctrl board. It is able to provide up to 5 A at 15 V.

Navi-Ctrl It is dedicated to record the flight data. This board mounts an AVR Atmel 16-bit microcontroller (25 MHz) and it communicates with the Flight-Ctrl through the Serial Peripherical Interface (SPI).

The original firmware has been modified in order to obtain flight data at a sampling frequency of 100 Hz. This data is stored in a microSD card during flight and downloaded for processing after landing.

4.2 Identification experiments

Identification experiments in flight can be carried out either manually, with the pilot exciting the dynamics of the helicopter using the remote control, or automatically, by implementing on-board functions to generate the input sequences for the experiments. In the case of a small-scale helicopter manual excitation is not sufficiently fast, so an automatic command generation function has been implemented. The input signal adopted for identification experiments is the so-called 3211 piece-wise constant sequence. The numbers used in the designation refer to the relative time intervals between control reversals. As discussed in Hamel and Kaletka [1997], this input sequence, developed at DLR, excites a wide frequency band within a short time period, so it is also suited for moderately unstable systems. Following the guideline in Klein and Morelli [2006], as the dominant dynamics of the quadrotor was expected to be around 5 rad/s, the duration of the second step has been set to half the period of the expected dominant mode. This choice led to a first step duration of 0.9 seconds, that is almost the maximum operable on a quadrotor without it flying too far away from trim. The width of the steps has been chosen asymmetric in order to obtain tests ending with almost null velocity. This maneuver has been repeated twice in order to get more data. The input signal used for the validation test is a so-called doublet, i.e., a sequence of two opposite steps of equal duration and amplitude. For the identification phase multiple datasets have been used: three double 3211 for an overall duration of approximately 20 seconds. For the cross-validation phase a double 3211 has been used for a duration of approximately 6.5 seconds. Finally, for the validation phase a doublet has been used for a duration of approximately 4 seconds. All the data has been filtered with a lowpass filter with a cutoff frequency of 5Hz. As an illustrative example, in Figure 2 the response of the vertical acceleration to a double 3211 applied to u_{col} is shown (the input command is expressed in terms of percentage of the trim value). Finally, note that while experiments exciting u_{col} have been carried out in open-loop, the identification of the response to the other control inputs has been carried out using closed-loop data.

5. EXPERIMENTAL RESULTS

Both model order and the tuning parameters of the identification algorithm (i.e., the position of the Laguerre pole

Input	Model order (n)	Laguerre pole (a)	Window length (p)
Collective	3	16	25
Pedal	3	16	10
Longitudinal	3	21	14
Lateral	3	15	8

Table 1. Selected tuning parameters of the algorithm for the identification of each model.

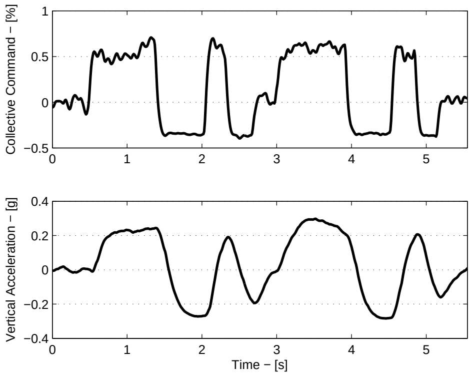

Fig. 2. Example of identification data. Top: 3211 collective excitation; bottom: response of vertical acceleration.

a and the past and future windows lengths p, f) have been selected using a cross-validation approach. More precisely, the model order has been selected by inspecting the singular values of $\Gamma^p \mathcal{K}^p \bar{Z}^{p,p}$ while the selection of a and p has been carried out by checking the 2-norm of the simulation error over the cross-validation dataset. The results of this step are shown in Table 1. Before the validation step, the identified models have been simplified by removing zeros at frequencies above the excitation bandwidth. Finally, the performance of the identified models has been checked by comparing the simulated outputs with the measured response to a doublet excitation applied on each of the control variables. The results of the validation experiments are presented in Figure 3 for the response of the vertical acceleration to the collective input, Figure 4 for the response of the yaw rate to the pedal input and Figures 5 and 6 for, respectively, the response of the pitch (roll) rate and of the longitudinal (lateral) acceleration to the longitudinal (lateral) input.

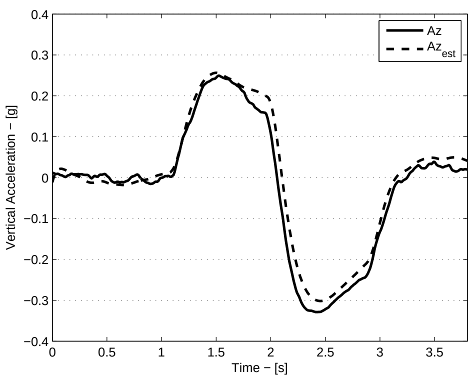

Fig. 3. Response of vertical acceleration to collective doublet (measured: solid line; estimated: dashed line).

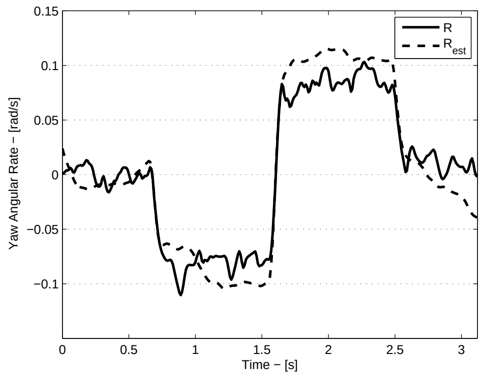

Fig. 4. Response of yaw rate to pedal doublet (measured: solid line; estimated: dashed line).

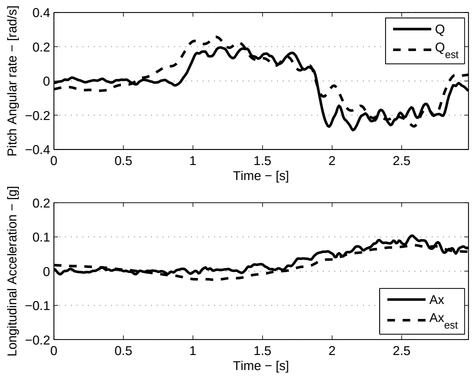

Fig. 5. Response of pitch rate (top) and longitudinal acceleration (bottom) to longitudinal cyclic doublet (measured: solid line; estimated: dashed line).

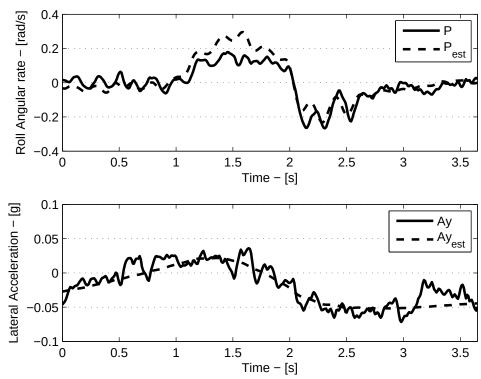

Fig. 6. Response of roll rate (top) and lateral acceleration (bottom) to lateral cyclic doublet (measured: solid line; estimated: dashed line).

Preprint submitted to 16th IFAC Symposium on System Identification.
Received November 14, 2011.

Finally, for the sake of completeness, the identified models are reported in Appendix A. Note, in passing, the significant symmetry between the models for lateral and longitudinal response, corresponding to the overall symmetry of the quadrotor platform, which therefore has been successfully captured by the identified models.

6. CONCLUDING REMARKS

The problem of black-box model identification of the dynamics of a quadrotor helicopter has been considered. A continuous-time subspace model identification approach has been adopted and an experimental case study has been carried out to demonstrate the feasibility of the approach.

REFERENCES

M. Bergamasco and M. Lovera. Continuous-time subspace identification in closed-loop. In *19th International Symposium on Mathematical Theory of Networks and Systems, Budapest, Hungary*, 2010a.

M. Bergamasco and M. Lovera. Continuous-time subspace identification in closed-loop using Laguerre filters. In *49th IEEE Conference on Decision and Control, Atlanta, USA*, 2010b.

M. Bergamasco and M. Lovera. Continuous-time predictor-based subspace identification using Laguerre filters. *IET Control Theory and Applications*, 5(7):856–867, 2011. Special issue on Continuous-time Model Identification.

S. Bittanti and M. Lovera. Identification of linear models for a hovering helicopter rotor. In *Proceedings of the 11th IFAC Symposium on system identification, Fukuoka, Japan*, 1997.

S. Bittanti and M. Lovera. Bootstrap-based estimates of uncertainty in subspace identification methods. *Automatica*, 36(11):1605–1615, 2000.

P. Castillo, R. Lozano, and A.E. Dzul. *Modelling and control of mini-flying machines*. Springer-Verlag New York Inc, 2005.

A. Chiuso and G. Picci. Consistency analysis of certain closed-loop subspace identification methods. *Automatica*, 41(3):377–391, 2005.

A. Das, K. Subbarao, and F. Lewis. Dynamic inversion with zero-dynamics stabilisation for quadrotor control. *IET Control Theory & Applications*, 3(3):303–314, 2009.

L. Derafa, T. Madani, and A. Benallegue. Dynamic modelling and experimental identification of four rotors helicopter parameters. In *IEEE International Conference on Industrial Technology*, pages 1834–1839. IEEE, 2006.

P. Hamel and J. Kaletka. Advances in rotorcraft system identification. *Progress in Aerospace Sciences*, 33(3-4): 259–284, 1997.

B. Huang, S.X. Ding, and S.J. Qin. Closed-loop subspace identification: an orthogonal projection approach. *Journal of Process Control*, 15(1):53–66, 2005.

R. Jategaonkar. *Flight Vehicle System Identification*. AIAA, 2006.

R. Johansson, M. Verhaegen, and C.T. Chou. Stochastic theory of continuous-time state-space identification. *IEEE Transactions on Signal Processing*, 47(1):41–51, 1999.

V. Klein and E.A. Morelli. *Aircraft System Identification: Theory And Practice*. AIAA, 2006.

M. La Civita, W. Messner, and T. Kanade. Modelling of small-scale helicopters with integrated first-principles ans system identification techniques. In *Proceedings of the 58th American Helicopter Society Annual Forum*, 2002.

P. Li and Postlethwaite I. Subspace and bootstrap-based techniques for helicopter model identification. *Journal of the American Helicopter Society*, 56(1):012002, 2011.

M. Lovera. Identification of MIMO state space models for helicopter dynamics. In *13th IFAC Symposium on System Identification, Rotterdam, The Nederlands*, 2003.

Y. Ohta. Realization of input-output maps using generalized orthonormal basis functions. *Systems & Control Letters*, 22(6):437–444, 2005.

Y. Ohta and T. Kawai. Continuous-time subspace system identification using generalized orthonormal basis functions. In *16th International Symposium on Mathematical Theory of Networks and Systems, Leuven, Belgium*, 2004.

M. Tischler and R. Remple. *Aircraft And Rotorcraft System Identification: Engineering Methods With Flight-test Examples*. AIAA, 2006.

P. Van Overschee and B. De Moor. *Subspace identification: theory, implementation, application*. Kluwer Academic Publishers, 1996.

M. Verhaegen. Identification of the deterministic part of MIMO state space models given in innovations form from input-output data. *Automatica*, 30(1):61–74, 1994.

M. Verhaegen and A. Varga. Some experience with the MOESP class of subspace model identification methods in identifying the BO105 helicopter. Technical Report TR R165-94, DLR, 1994.

M. Verhaegen and V. Verdult. *Filtering and System Identification: A Least Squares Approach*. Cambridge University Press, 2007.

K. Zhou, J. Doyle, and K. Glover. *Robust and optimal control*. Prentice Hall, 1996.

Appendix A. IDENTIFIED MODELS

$$G_{col}(s) = \frac{a_z}{u_{col}} = \frac{1.2498(s+0.3451)}{(s+16.49)(s+5.309)(s+1.933)}$$

$$G_{yaw}(s) = \frac{r}{u_{ped}} = \frac{0.077646(s+5.475)(s-0.2086)}{(s+11.03)(s^2+0.2838s+0.06947)}$$

$$G_{lon}(s) = \begin{bmatrix} \dfrac{q}{u_{lon}} \\ \dfrac{a_x}{u_{lon}} \end{bmatrix} = \begin{bmatrix} \dfrac{0.22016(s+0.2579)(s-0.2596)}{(s+1.865)(s^2-1.285s+8.067)} \\ \dfrac{-0.011659(s-3.271)(s+3.681)}{(s+1.865)(s^2-1.285s+8.067)} \end{bmatrix}$$

$$G_{lat}(s) = \begin{bmatrix} \dfrac{p}{u_{lat}} \\ \dfrac{a_y}{u_{lat}} \end{bmatrix} = \begin{bmatrix} \dfrac{-0.20194(s^2+0.09235s+0.2532)}{(s+1.82)(s^2-1.388s+10.02)} \\ \dfrac{-0.00359(s-9.182)(s+4.164)}{(s+1.82)(s^2-1.388s+10.02)} \end{bmatrix}.$$